HHS Public Access

Author manuscript

Nat Struct Mol Biol. Author manuscript; available in PMC 2012 January 01.

Published in final edited form as:

Nat Struct Mol Biol. ; 18(7): 813–821. doi:10.1038/nsmb.2075.

Mechanism and function of synaptotagmin-mediated membrane apposition

Enfu Hui[1,2,3], **Jon D. Gaffaney**[1,3], **Zhao Wang**[1], **Colin P. Johnson**[1], **Chantell S. Evans**[1], and **Edwin R. Chapman**[1]

[1]Howard Hughes Medical Institute and Department of Neuroscience, University of Wisconsin, 1300 University Avenue, SMI 129, Madison, WI, 53706

SUMMARY

Synaptotagmin-I (syt) is a Ca^{2+} sensor that triggers synchronous neurotransmitter release. The first documented biochemical property of syt was its ability to aggregate membranes in response to Ca^{2+}. However, the mechanism and function of syt-mediated membrane aggregation are poorly understood. Here, we demonstrate that syt-mediated vesicle aggregation is driven by *trans* interactions between syt molecules bound to different membranes. We observed a strong correlation between the ability of Ca^{2+}-syt to aggregate vesicles and to stimulate SNARE-mediated membrane fusion. Moreover, artificial aggregation of membranes - using non-syt proteins - also efficiently promoted fusion of SNARE-bearing liposomes. Finally, using a modified fusion assay, we observed that syt drives the assembly of otherwise non-fusogenic individual t-SNARE proteins into fusion competent heterodimers, in an aggregation-independent manner. Thus, membrane aggregation and t-SNARE assembly appear to be two key aspects of Ca^{2+}-syt-regulated, SNARE-catalyzed fusion reactions.

INTRODUCTION

Communication between neurons relies on Ca^{2+}-triggered exocytosis of synaptic vesicles. Fusion of synaptic vesicles with the plasma membrane is mediated by soluble NSF attachment protein receptors (SNAREs). The Ca^{2+} sensitivity of this process is mainly conferred by syt, a vesicle protein that harbors tandem C2 domains, C2A and C2B. Genetic ablation of syt in mice or *Drosophila* disrupted the tight temporal coupling between Ca^{2+} influx and neurotransmitter release[1]. In addition, the recombinant cytoplasmic domain of syt (C2AB) imparts Ca^{2+} sensitivity to *in vitro* fusion assays using vesicle (v-; synaptobrevin 2) and target membrane (t-; syntaxin 1A and SNAP-25B) SNARE-bearing liposomes - addition

Correspondence should be addressed to E.R.C. (chapman@wisc.edu)..

[2]Present address: Department of Molecular and Cellular Pharmacology, University of California, San Francisco, 600-16th street, San Francisco, CA, 94158

[3]These authors contributed equally to this work.

AUTHOR CONTRIBUTIONS E.R.C conceived of and supervised the project. E.H., J.D.G and E.R.C. designed the experiments and wrote the manuscript; E.H. conducted all the aggregation assays on syt proteins and cPLA2-C2, membrane penetration assays, and FRET-based membrane binding assays; J.D.G. conducted all the fusion assays on syt proteins and cPLA2-C2, and performed experiments for Fig. 6 with Z.W.; Z.W carried out experiments for Fig. 9; C.P.J conducted avdin-biotin mediated aggregation and fusion assays in Fig. 2d, i and Fig. 8e–h; C.S.E carried out experiments in Supplementary Fig. 8.

of C2AB greatly accelerates membrane merger in response to Ca^{2+}, but suppresses fusion in the absence of Ca^{2+}[2,3]. While the role of syt as a Ca^{2+} sensor has become generally accepted, the mechanism by which syt regulates SNARE-catalyzed fusion remains poorly understood and is the subject of intensive study.

One of the first documented activities of syt was its ability to aggregate membranes in response to Ca^{2+}[4,5]. Subsequent studies demonstrated that the C2AB domain of syt efficiently aggregated chromaffin granules as well as artificial liposomes that harbor the anionic phospholipid, phosphatidylserine (PS)[6,7]. A number of studies have re-visited this issue and confirmed the ability of syt to aggregate membranes[8–12], but the underlying mechanism and its physiological role is a subject of debate.

Damer et al. postulated that aggregation is due to the interaction between syt molecules that are bound to distinct membranes[7]. This model was based on the finding that Ca^{2+} triggers the oligomerization of syt even in the absence of membranes. However, Ca^{2+}-triggered oligomerization of syt in solution might be an artifact that involves the presence of bound nucleic acid contaminants[13–15]. Subsequently, based on data obtained with nucleic acid-free materials, Arac et al. proposed that syt-mediated aggregation is due to multivalent interactions of the C2B domain with membranes[8]. However, a separate study found that the isolated C2B domain failed to aggregate liposomes, and that only tandem C2-domain proteins are able to cluster vesicles, proposing that syt-mediated aggregation occurs when C2A and C2B engage two different membranes[9].

In response to Ca^{2+}, both C2 domains of syt rapidly penetrate into the hydrophobic core of membranes that harbor anionic phospholipids[16,17], and this penetration activity is essential for syt to stimulate membrane fusion[18]. The partial insertion of C2AB into the target membrane[3] induces positive curvature to the lipid bilayer facilitating fusion[19,20]. Although it has been proposed that C2AB-mediated membrane aggregation is also important for syt to stimulate membrane fusion[8], direct evidence to support this idea is lacking. A recent study showed that R398, 399Q mutations within the C2B domain impair both membrane aggregation and synaptic transmission[21]. However, mutation of these two residues also compromises the ability of syt to interact with t-SNAREs[11] and, potentially, the ability of syt to bend membranes.

In the present study, we investigated the mechanism of syt-regulated vesicle aggregation. We demonstrate that C2AB, as well as each of its isolated C2-domains, aggregate vesicles in response to Ca^{2+}. FRET analysis revealed that only the Ca^{2+} binding loops of the C2B domain bind lipids, inconsistent with previous observations[8]. Using a variety of approaches, we report that syt-mediated membrane aggregation occurs through *trans*-association of syt molecules bound to distinct membranes. Surprisingly, aggregation of SNARE-bearing liposomes through the use of non-syt molecules resulted in dramatically enhanced fusion as well; however, only Ca^{2+}-syt was able to stimulate fusion when unassembled t-SNAREs were used, emphasizing its unique ability to assemble SNAP-25 and syntaxin into fusion competent SNARE complexes[10].

RESULTS

Syt mediates aggregation of liposomes in response to Ca^{2+}

Increases in the turbidity of vesicle suspensions are routinely used as an index of vesicle aggregation[22]. We used this method to characterize syt-mediated vesicle aggregation by monitoring changes in turbidity over time after sequential addition of the C2AB domain of syt, Ca^{2+} and excess EGTA to chelate Ca^{2+} (Fig. 1). Using protein-free, liposomes, we found that C2AB aggregates vesicles with rapid kinetics in response to Ca^{2+} (τ = 49.8 s). C2AB-mediated vesicle aggregation did not occur prior to the addition of Ca^{2+}, and was readily reversed by excess EGTA (Fig. 1a); hence, syt-mediated vesicle aggregation is strictly Ca^{2+} dependent.

We next determined whether the presence of SNARE proteins affects Ca^{2+}-C2AB-mediated aggregation, by using small unilamellar vesicles (SUVs) that harbor reconstituted t-SNARE heterodimers (designated as Tr) or v-SNAREs (designated as Vr) (Fig. 1b and 1c). In both cases, C2AB aggregated SNARE-bearing vesicles in a Ca^{2+}-dependent manner, with similar kinetics as when protein free vesicles were utilized (τ = 44.4 s and 58.8 s for Tr and Vr, respectively). Finally, we analyzed the ability of C2AB to aggregate vesicles that contain both Tr and Vr, and found that syt induced a rapid turbidity increase of these samples in response to Ca^{2+} (τ = 54.0 s) (Fig. 1d). Interestingly, the increase in turbidity was only partially reversed by addition of excess EGTA; the residual increase in turbidity is likely to be due to SNARE-mediated fusion of Tr and Vr.

Aggregation induced by synaptotagmin, polylysine, or avidin-biotin

Recent studies of syt-mediated aggregation have resulted in contradictory findings[8,9], which might be due to the use of different protein-to-lipid ratios. To clarify this issue, we quantitatively analyzed the liposome aggregation activity of syt, as a function of [syt] and [lipid].

In the presence of Ca^{2+}, the turbidity increased monotonically as a function of [C2AB], exhibiting two phases with an inflection point at ~10 μM (Fig. 2a, closed circles). In the absence of Ca^{2+}, C2AB failed to aggregate vesicles at all concentrations tested. Notably, C2AB alone - in the absence of lipids - underwent Ca^{2+}-dependent aggregation at concentrations ≥10 μM (Fig. 2a, open circles). Thus, the second phase of the turbidity increase was likely due to aggregation of free C2AB molecules that only occurred at high protein concentrations. Indeed, by subtracting the protein-alone aggregation signals from those of the protein-liposomes mixtures, we obtained a saturable sigmoidal dose-response for C2AB-mediated liposome aggregation (Fig. 2b).

Next, we compared syt with two other aggregating proteins: poly-D-lysine and avidin. Polylysine is able to cross-link multiple membranes through electrostatic attractions between its basic side chains and the head-groups of acidic phospholipids. Tetrameric avidin binds up to four biotin molecules with femto-molar affinity[23], enabling it to crosslink biotinylated membranes.

Polylysine-mediated aggregation of liposomes exhibited a bell-shape dependence on [polylysine] (Fig. 2c), consistent with previous work examining the aggregation of chromaffin granules[7]. Titration of avidin onto biotinylated vesicles also produced a bell-shaped aggregation response (Fig. 2d). These bell-shaped dose curves are likely due to binding site saturation: excess protein would result in depletion of binding sites rendering these molecules unable to engage multiple liposomes. By contrast, titration of C2AB resulted in a sigmoidal response (Fig. 2b). Persistent membrane aggregation at high C2AB-to-lipid ratios (Fig. 2e) can only be mediated by self-association of C2AB molecules that are bound to distinct membranes. Finally, no difference in the turbidity was observed between buffer control and high [polylysine] or [avidin] (data not shown).

Conversely, we also titrated the lipid and monitored aggregation mediated by Ca^{2+}-C2AB, polylysine, or avidin-biotin. Under these conditions, C2AB-mediated aggregation exhibited a bell-shaped curve (Fig. 2f, g), whereas polylysine-mediated aggregation displayed a saturable sigmoidal dose-response (Fig. 2h). Avidin-mediated aggregation resembled polylysine-mediated aggregation except for a slight decrease in aggregation at relatively high [avidin] (Fig. 2i). These results strongly suggest that C2AB utilizes a fundamentally different mechanism to aggregate vesicles than polylysine or avidin.

Mutational analyses of syt-mediated liposome aggregation

To gain further insights into the mechanism by which syt aggregates membranes, we compared the vesicle aggregation activities of several C2AB mutants (Fig. 3). We note that in Fig. 2a vesicle aggregation strongly depends on C2AB concentration. Therefore, we analyzed the aggregation activity of the mutants as a function of protein concentration (Fig. 3). We found that neutralization of the Ca^{2+} ligands within either C2A or C2B, which renders the domain unable to bind Ca^{2+} and penetrate membranes, increased the protein requirement for aggregation by ~10-fold and ~2-fold, respectively. Simultaneous neutralization of Ca^{2+} ligands in both C2 domains (D230, 232, 363, 365N), completely abolished the aggregation activity of syt.

We next examined the abilities of isolated C2 domains to aggregate vesicles. The C2B domain was observed to aggregate liposomes at ≥ 5 μM, whereas isolated C2A began to aggregate liposomes at >10 μM; ~25-fold and ~50-fold higher than for C2AB, respectively. The vesicle aggregation activities of tandem C2A (C2AA) or C2B domains (C2BB) revealed that tethering of C2 domains greatly enhanced their abilities to aggregate vesicles (threshold concentrations: ~0.5 μM for C2AA and ~0.2 μM for C2BB) (Fig. 3). We note that aggregation of the proteins alone was negligible at the concentrations reported in Fig. 3 (Supplementary Fig. 1), therefore the uncorrected aggregation signals were used. These results were somewhat surprising given previous work showing that C2BB binds membranes less avidly than C2AA[20]. In addition, the large Hill coefficients for C2AA- and C2BB-mediated aggregation (4.0 and 4.9 respectively) indicate that cross-linking of membranes requires the cooperative action of multiple copies of protein and cannot be explained by individual domains penetrating different membranes. The relative aggregation activities for these constructs suggest that the C2B rather than the C2A domain has a greater

propensity to oligomerize. Furthermore, these data support the idea that oligomerization of C2 domains at least partially contributes to the vesicle aggregation activity of syt.

The `bottom' of the C2B domain does not bind to membranes

Although we found that Ca^{2+}-C2B-mediated aggregation does not occur at low protein concentrations, which is in contrast to a previous report[8], we confirmed that the R398, 399Q mutations inhibit the membrane aggregation activity of C2AB and C2B (Fig. 3). In our hands, neutralization of Arg398, 399 increased the aggregation threshold for C2AB from ~0.2 μM to ~1 μM, and rendered C2B unable to aggregate membranes at even 20 μM protein. Interestingly, residues Arg398, 399 are located at the bottom of the C2B domain, opposite the Ca^{2+} binding, membrane penetration loops. Arac et al. proposed that Arg398 penetrates PS-harboring membranes in response to Ca^{2+}, thereby enabling a single copy of C2B to bridge two membranes[8]. However, our dose-response experiments (Fig. 2) suggest that aggregation is unlikely to be mediated by a single copy of C2B, arguing against the presence of a second lipid binding site.

We directly determined whether C2B engages PS harboring membranes via multiple surfaces by using an environmentally sensitive fluorescence probe. Single cysteine mutations were introduced at different locations throughout the C2B domain and stoichiometrically labeled with NBD (Fig. 4a). Because C2AB-mediated aggregation is strongly dependent on [protein] (Fig. 3), we selected two [C2AB] for the fluorescence studies: 0.3 μM, at which C2AB efficiently aggregates liposomes, and 0.1 μM, which is below the threshold concentration for liposome aggregation. Therefore, multiple membrane binding sites should exist only when the concentration exceeds the aggregation threshold. We found that at 0.3 μM, NBD probes that are introduced to the tips of the Ca^{2+} binding loop 1 or 3 (V304C or I367C) exhibited dramatic increases in intensity as well as blue shifts in their spectra in response to Ca^{2+} (Fig. 4b, d), consistent with the idea that these residues insert into the nonpolar phase of the bilayer[24,25]. In addition, loop 2 of C2B also appeared to penetrate membranes in response to Ca^{2+} (Fig. 4c). By contrast, none of the other NBD-labeled mutants showed any fluorescence changes in response to Ca^{2+} (Fig. 4e–l). At 0.1 μM, a condition in which vesicle aggregation was undetectable (Fig. 3), we observed a similar result, i.e., only V304C, N333C and I367C penetrate membranes in response to Ca^{2+} (Supplementary Fig. 2). Hence, the membrane penetration activity appears to be unique to the three loops that protrude from the `top' of each C2-domain of syt.

While the fluorescence experiments described above demonstrate that Arg398, 399 do not penetrate into the membrane, it remains possible that these basic residues superficially bind to the negatively charged head-groups of PS. To address this possibility, we next measured Förster resonance energy transfer (FRET) between NBD-labeled C2AB (Fig. 4a) and rhodamine that was conjugated to the head-group of phosphatidylethanolamine (PE) within membranes. When NBD was placed at the tip of the Ca^{2+} binding loops, robust energy transfer was detected (Fig. 5a–c). Excitation of NBD resulted in a marked increase in the rhodamine fluorescence (λ_{max}~580 nm), and a concomitant decrease in NBD fluorescence (λ_{max} ~530 nm), as compared to control liposomes that lacked rhodamine. Ca^{2+}-dependent FRET signals were considerably weaker when NBD was moved to other surfaces of the

C2B domain (Fig. 5d–k). Similar results were observed when [C2AB] below the aggregation threshold (0.1 μM, Supplementary Fig. 3) were used. These findings further support the conclusion that the Ca^{2+}-binding loops comprise the only region of C2B that directly interacts with PS-containing membranes. The weak FRET signals that were observed when NBD was placed on other surfaces of C2B are not surprising since longest dimension of the C2B domain (~5 nm) is similar to the Förster radius for the NBD-rhodamine FRET pair (~5.6 nm[26]).

Because the presence of an adjacent C2A domain greatly enhances the membrane insertion activity of C2B[25,27], we then repeated the NBD-reporter penetration experiments described above but in the context of isolated C2B. Again, only the Ca^{2+}-binding loops of C2B penetrate into membranes (Supplementary Figs. 4 and 5). We also confirmed these results by measuring FRET between NBD-labeled isolated C2B and rhodamine-bearing liposomes (Supplementary Figs. 6 and 7).

Taken together, the fluorescence measurements demonstrate that a single C2B molecule is unable to engage multiple membranes. In addition, we also discovered that neutralization of Arg398, 399 did not affect the membrane penetration activity of the Ca^{2+}-binding loops (Supplementary Fig. 8). Thus, the positively charged residues at the bottom of C2B neither directly interact with membranes, nor are needed to support the membrane penetration activity of this domain.

C2AB induced aggregation occurs through *trans* interactions

We reiterate that the ability of C2AB to aggregate membranes at high protein concentrations, unlike polylysine and biotin-avidin, suggest it uses a distinctly different mechanism to crosslink liposomes (Fig. 2). In addition, our fluorescence measurements demonstrate that a single copy of C2AB binds to only one membrane (Figs. 4 and 5). Thus, the ability of C2AB to mediate membrane aggregation is likely to involve intermolecular interactions. Indeed, electron and atomic force microscopy experiments revealed that C2AB molecules can oligomerize on membrane surfaces and that the C2B domain appears to be essential in this process[15,28]. Therefore, we postulate that membrane-bound C2ABs are able to self-associate, *in trans*, leading to membrane aggregation.

To test this idea, we prepared two populations of liposomes: biotin containing vesicles, which can be captured with avidin beads, and vesicles that harbor dansyl, which serves as a fluorescence reporter (Fig. 6). C2AB binds to PS-containing liposomes with sub-nM affinity and has an extremely slow off-rate in the presence of Ca^{2+}[29]. By preincubating C2AB and Ca^{2+} with two distinct sets of vesicles one can effectively pin the protein to a vesicle. Indeed, we found that virtually all of the C2AB was absorbed onto liposomes upon mixing (Fig. 6a). To determine whether copies of C2AB from these two distinct vesicle populations bind to each other, we mixed these two sets of C2AB-coated vesicles together in the presence of Ca^{2+}. Robust dansyl fluorescence was detected after extensive washing of the avidin beads (Fig. 6c, **black bar, #3**), suggesting that C2AB-coated dansyl vesicles bound to C2AB-coated biotin vesicles. Importantly, omission of C2AB from either set of vesicles completely abolished the co-precipitation of these two sets of vesicles (Fig 6c, **black bars, #1 and #4**). This result demonstrates that C2AB must be present on both membranes to

support membrane aggregation. Thus, a single copy (layer) of C2AB cannot crosslink multiple vesicles. As expected, chelation of Ca^{2+} by EGTA, which dissociated C2AB from membranes, blocked the vesicle co-precipitation (Fig. 6c, **open bars**).

We then directly addressed the question of whether the R398, 399Q mutations, which strongly inhibit vesicle aggregation activity (Fig. 3), compromise the *trans*-interactions between copies of membrane bound C2AB. Similar to wild-type C2AB, this mutant was efficiently prepinned onto PS-containing liposomes (Fig. 6a). However, the two sets of protein-coated liposomes failed to interact with each other upon mixing (Fig. 6c, **grey bar, #3**).

Taken together, these data strongly support the idea that copies of membrane-bound syt are able to associate with each other, *in trans*, to mediate liposome aggregation, and that basic residues at the bottom of C2B domain (Arg398 and Arg399) play an important role in this interaction. This model is consistent with a previous study in which C2AB forms ring-like oligomers with an axial dimension of 11 nm, which is roughly twice of the longest dimension of a single C2 domain (~5 nm)[15]. Moreover, a more recent study found that C2AB-mediated membrane aggregation results in a distance of ~9 nm between apposed membranes[9]. Further experiments will be required to determine the affinity, stoichiometry and detailed structure of membrane-bound syt oligomers.

Synaptotagmin promotes fusion, in part, by aggregating membranes

Membrane fusion is preceded by close membrane apposition. Thus, it is tempting to speculate that C2AB's ability to aggregate vesicles might play a role in stimulating membrane fusion in response to Ca^{2+}. To monitor fusion, the lipid-conjugated NBD-rhodamine FRET pair were incorporated into donor vesicles. Fusion between donor v- and acceptor t-SNARE vesicles results in dilution of NBD-rhodamine FRET pair and dequenching of the NBD fluorescence[2,30].

To determine whether there is a correlation between the ability of syt to cluster vesicles and to stimulate fusion, the C2AB domain was titrated into both the fusion (Fig. 7a) and aggregation assays. Since the aggregating activity of syt is strongly dependent on the [lipid] (Fig. 2f), we utilized the same [lipid] in both assays (based on previously determined lipid concentrations for Tr and Vr vesicles[20]). When the two plots were overlaid (Fig. 7b), we observed a strong correlation between the extent of fusion and the degree of vesicle aggregation. Positive correlations were also observed for all of the mutant forms of syt that were tested (Fig. 7c–j). These findings strongly suggest that membrane aggregation contributes to the ability of syt to regulate fusion of SNARE-bearing vesicles.

The importance of charged residues (Arg398, 399) for aggregation suggests that syt-mediated liposome aggregation involves intermolecular electrostatic interactions. Such contacts would be disrupted by high concentrations of salt. Indeed, increasing [KCl] to ≥200 mM completely abolished both C2AB-mediated aggregation (Supplementary Fig. 9a, b) and C2AB-regulated, SNARE-catalyzed fusion (Supplementary Fig. 9c, d) (note: increasing [salt] had relatively small effects on fusion mediated by SNAREs alone; Supplementary Fig. 9e, f). The strikingly similar salt sensitivity of aggregation and fusion further support the

conclusion that vesicle aggregation is a key step during Ca^{2+}–syt-regulated fusion of SNARE-bearing liposomes.

We next determined whether membrane aggregation alone is sufficient to promote SNARE-mediated fusion. To address this question, we chose to use the C2 domain from cytosolic phospholipase A2 ($cPLA_2$), an enzyme which hydrolyzes phospholipids to release fatty acids and lysophospholipids[31]. The C2 domain of $cPLA_2$ (designated as $cPLA_2$-C2) is able to aggregate membranes in response to Ca^{2+} (Fig. 8a) yet fails to interact with SNARE proteins (data not shown). We found that $cPLA_2$-C2 efficiently accelerates fusion of SNARE-bearing SUVs in response to Ca^{2+} (Fig. 8b). Similar to the C2 domains of syt, the ability of $cPLA_2$-C2 to mediate aggregation is correlated with its ability to promote SNARE-mediated fusion (Fig. 8c, d).

To further test the effect of aggregation on fusion, we took advantage of the avidin-biotin-PE system detailed above (Fig. 2d, i) to induce aggregation of SNARE-bearing vesicles (Fig. 8e). Strikingly, addition of avidin also induced a rapid burst in the fusion signal (Fig. 8f). Again, the vesicle aggregation activity of avidin is correlated with its ability to stimulate SNARE-catalyzed fusion (Fig. 8g, h).

Together, these results strongly suggest that aggregation is sufficient to promote fusion of t-SNARE heterodimer-bearing vesicles with v-SNARE vesicles, when highly curved SUVs are used. Membrane aggregation might serve to bring v- and t-SNARE-bearing vesicles into close proximity to promote the assembly of cognate *trans*-SNARE complexes.

Decoupling synaptotagmin-t-SNARE binding from fusion and aggregation

Syt binds to t-SNARE heterodimers in a Ca^{2+}-promoted manner[2,32,33], and considerable evidence suggests that this interaction is important for regulated fusion[34]. The Ca^{2+}-independent component of syt-SNARE interactions enable syt to suppress fusion prior to Ca^{2+} arrival[3], whereas Ca^{2+}-dependent component of syt-t-SNARE interactions appear to be important for syt to promote fusion in response to Ca^{2+}[2,10,32,33,35–37]. However, the tight correlation between membrane aggregation and fusion raised the question of whether the interaction of syt with t-SNARE heterodimers is important for the regulation of fusion. To address this, we compared the Ca^{2+} dose-responses for membrane aggregation (Supplementary Fig. 10a), fusion (Supplementary Fig. 10b,c) and t-SNARE binding (Supplementary Fig. 10d,e). We found that aggregation and fusion were again tightly correlated, having similar $[Ca^{2+}]_{1/2}$ values (~300 μM). In contrast, C2AB-t-SNARE interactions exhibited a bi-modal Ca^{2+} dependence, occurring before the onset of fusion ($[Ca^{2+}]_{1/2}$: ~60 μM) and diminishing at Ca^{2+} levels above 1 mM (Supplementary Fig. 10h). These findings suggest that the Ca^{2+}-dependent component for binding of syt to preformed t-SNARE heterodimers is not obligatory for syt to stimulate SNARE-mediated fusion to at least some degree. The Ca^{2+} dose-response for C2AB-membrane association was also analyzed in parallel via a co-sedimentation assay (Supplementary Fig. 10f, g). Interestingly, this Ca^{2+} dose-response curve was left-shifted ($[Ca^{2+}]_{1/2}$: 145 ± 23 μM) as compared to the curve that describes membrane aggregation (Supplementary Fig. 10h), indicating that aggregation requires a second Ca^{2+}-dependent step (e.g., oligomerization of C2AB) following membrane association.

Synaptotagmin can assemble fusion competent t-SNARE heterodimers

Syt not only interacts with preassembled t-SNARE heterodimers, but also binds to individual t-SNAREs (syntaxin or SNAP-25) stoichiometrically, in a rapid Ca^{2+}-promoted manner[32,38–41]. In particular, Ca^{2+}-C2AB has been shown to drive the assembly of soluble SNAP-25 onto membrane-embedded syntaxin to form stable fusion competent t-SNARE heterodimers[10]. In the context of this study, it remained possible that C2AB stimulated fusion by merely aggregating membranes.

To directly address the functional significance of syt-mediated assembly of t-SNARE heterodimers, we compared the abilities of C2AB, $cPLA_2$-C2, and avidin–biotin to stimulate fusion between syntaxin bearing vesicles (SYXr) and Vr, in the presence of soluble SNAP-25. In these experiments, both SYXr and Vr vesicles harbor PS and biotin so that they can be aggregated by either C2AB, $cPLA_2$-C2, or avidin. Addition of Ca^{2+}-C2AB to SYXr, Vr, and SNAP-25 greatly enhanced membrane fusion. In contrast, fusion between Vr and SYXr with SNAP-25 alone or in the presence of $cPLA_2$-C2 or avidin was not observed (Fig. 9a). This is consistent with the finding that syntaxin and SNAP-25 fail to assemble and drive fusion when purified separately[30] and that $cPLA_2$-C2 and avidin do not interact with t-SNAREs (data not shown). Thus, aggregation alone is not sufficient to stimulate fusion between vesicles that harbor unassembled t-SNAREs. These findings uncover an additional step performed by syt to promote membrane fusion, i.e., syt drives the assembly of the otherwise non-fusogenic syntaxin and SNAP-25 into fusion competent t-SNARE heterodimers.

DISCUSSION

In the present study, we characterize the mechanism of syt-mediated membrane aggregation. Our data support a model in which syt-mediated aggregation relies on both syt-membrane interactions and intermolecular interactions. In this model, copies of membrane-bound syt - from different membranes - bind to each other via *trans* protein-protein interactions (Fig. 6). This interaction is mediated through residues Arg398, 399 located on the `bottom' of the C2B domain. It is likely these basic residues form a positively charged patch that interacts with acidic surfaces found on a different C2B molecule. The combination of membrane binding and protein oligomerization could bring the membranes into close apposition enabling *trans*-SNARE interactions to occur more efficiently. Interestingly, annexin IV has been shown to undergo two modes of oligomerization: *cis*-oligomerization followed by *trans*-oligomerization and liposome aggregation[42]. This model suffices to explain most of our data and is consistent with the inter-membrane spacing of ~9 nm for C2AB-aggregated membranes[9]. Thus, syt and annexin IV are self-adhesive membrane binding molecules.

A dramatic enhancement of vesicle aggregation was observed when C2-domains were tethered together (Fig. 3). The C2AA and C2BB constructs can be viewed as preformed dimers of C2A and C2B, presumably facilitating the assembly of higher order oligomers. Moreover, tethered C2-domains (i.e. C2AB, C2AA, and C2BB) bind membranes with much higher affinity than isolated C2 domains[20] and are therefore more likely to partition to membranes to reach the threshold density for oligomerization. Binding of C2AB to membranes serves to concentrate it on a two-dimensional membrane surface, allowing

oligomerization to occur at a lower bulk [protein]. This may explain why the threshold concentrations for syt-mediated liposome aggregation are much lower than for syt-syt oligomerization in solution (Fig. 2a and Supplementary Fig. 1).

Two previous models for membrane aggregation were proposed; the first suggested that the C2B domain contains multiple membrane binding surfaces[8], while the second postulated that the C2A and C2B domains bind to the vesicle and target membranes, respectively[9]. Using membrane penetration and FRET assays we have demonstrated that the C2B and tethered C2AB domains only bind lipids through their Ca^{2+} binding loops (Fig. 4, 5 and Supplementary Fig. 2–7), arguing against a multivalent model. In addition, the observation that the isolated C2B domain aggregates membranes argues directly against the tethering model. Furthermore, neither of the previous models could explain the highly cooperative nature of C2AB-mediated aggregation (Fig. 3) or that it does not require the presence of `naked' membrane (Fig. 2c, d).

We have also demonstrated that syt stimulates the fusion of SNARE-bearing vesicles, at least in part, by aggregating vesicles together. By varying [syt] (Fig. 7) or changing the ionic strength (Supplementary Fig. 9), we discovered that stimulated fusion only occurs when syt aggregates vesicles. A tight correlation between fusion and liposome aggregation was observed for a wide range of syt mutants. To our knowledge, this is the first direct evidence that membrane aggregation activity is required for syt to stimulate fusion of SNARE-bearing vesicles. Indeed, the protein dose-responses for aggregation (Fig. 3) allow us to reliably predict the relative ability of each syt mutant to promote fusion of SNARE-bearing SUVs (Fig. 7).

Surprisingly, avidin (acting through biotinylated lipids) and $cPLA_2$-C2, which do not bind SNARE proteins, can mediate vesicle aggregation and fusion (Fig. 8b, f). These results suggest that membrane aggregation is sufficient to promote fusion; however, no fusion was observed when protein free liposomes were used (data not shown), indicating aggregation-induced fusion is strictly dependent on the presence of SNARE proteins. A likely explanation for these effects is that holding membranes together, via aggregation, increases the probability of SNARE pairing, thus helping to initiate the assembly of *trans*-SNARE complexes. Alternatively, by potentially shortening the intermembrane distance, aggregation could promote complete zippering of partially assembled SNARE complexes. Oligomerization-mediated vesicle aggregation can certainly occur in *in vitro* fusion assays: mixing two populations of C2AB-coated liposomes leads to *trans*-aggregation of these vesicles (Fig. 6). Such oligomerization-mediated membrane apposition might also occur *in vivo*, as ~30% of syt molecules reside in the plasma membrane[43]. Consistent with this model is the finding that the R398, 399Q mutations, which disrupt *trans*-oligomerization (Fig. 6c), drastically impair the function of syt during neurotransmitter release *in vivo*[21].

Considerable evidence supports the idea that syt also regulates membrane fusion, at least in part, by directly engaging t-SNARE heterodimers[34]. However, in the current study, we have shown that either avidin or $cPLA_2$-C2, which do not interact with SNAREs, efficiently stimulate fusion in cases where t-SNARE heterodimers are pre-assembled prior to reconstitution (Fig. 8b, f). These data clearly indicate that the interaction between syt and

pre-formed t-SNARE heterodimers is not absolutely required for stimulated fusion *in vitro*. However, data presented here also suggest that syt-SNARE interactions can promote fusion after the aggregation step. For example, although C2AA, C2AB (D230, 323N), C2AB (D363, 365N), and C2AB (R398, 399Q) display strong aggregation activity at high concentrations, these mutants exhibit diminished fusion activity (Fig. 7e, g, h, and i), which correlate with their compromised t-SNARE binding activity as reported previously[11,20,44].

Little is known regarding how and when the t-SNAREs syntaxin and SNAP-25 assemble into heterodimers in cells. In conventional fusion assays, preassembled t-SNAREs heterodimers were used because soluble SNAP-25, added to reconstituted syntaxin vesicles, failed to assemble into fusion competent t-SNARE heterodimers[30]. Ca^{2+}-C2AB was recently found to promote the assembly of syntaxin and SNAP-25 into fusogenic t-SNARE heterodimers[10]. This finding revealed a new function of syt during early stages of SNARE assembly, and is consistent with studies of permeabilized PC12 cells indicating that SNARE complex assembly is triggered by Ca^{2+}[45]. However, it was not clear whether the stimulatory effect of syt was due to its ability to drive t-SNARE assembly or to aggregate membranes. In the current study, we successfully dissociated these two activities using proteins that aggregate membranes but do not interact with SNAREs. When the target membrane harbors pre-formed syntaxin-SNAP-25 heterodimers, membrane aggregation is sufficient to stimulate fusion; in contrast, when unassembled t-SNAREs (SYXr plus soluble SNAP-25) were employed, membrane aggregation alone failed to promote fusion (Fig. 9a). Therefore, we propose a working model for syt in reconstituted fusion assays in which syt promotes SNARE-mediated fusion by directly affecting the structure and function of SNARE proteins (Fig. 9b).

The formation of fusogenic *trans*-SNARE complexes is likely to occur in a two-step process: first, syntaxin and SNAP-25 assemble into t-SNARE heterodimers, which then pair with the v-SNARE synaptobrevin to form ternary *trans*-SNARE complexes. The data presented here suggest that Ca^{2+}-syt promotes the first step by directly driving the assembly of t-SNARE heterodimers, and then facilitates the second step by juxtaposing t- and v-membranes through its aggregation activity.

METHODS

Materials

Synthetic 1,2-dioleoyl-sn-glycero-3-phospho-l-serine (phosphatidylserine, PS), 1-palmitoyl-2-oleoyl-sn-glycero-3-phosphocholine (phosphatidylcholine, PC), 1-palmitoyl-2-oleoyl-sn-glycero-3-phosphoethanolamine (phosphatidylethanolamine, PE), 1,2-dioleoyl-sn-glycero-3-phosphoethanolamine-N-(biotinyl) (18:1 Biotin-PE), 1,2-dipalmitoyl-sn-glycero-3-phospho-ethanolamine-N-(7-nitro-2-1,3-benzoxadiazol-4-yl) (NBD-PE) and N-(lissamine rhodamine B sulfonyl)-1,2-dipalmitoyl-sn-glycero-3-phosphoethanolamine (rhodamine-PE) were purchased from Avanti Polar Lipids. N,N'-dimethyl-N-(iodoacetyl)-N'-(7-nitrobenz-2-oxa-1,3-diazol-4-yl)ethylenediamine (IANBD amide) were obtained from Molecular Probes. Poly-D-lysine hydrobromide (Molecular Weight: 500–550 kDa) was obtained from BD Biosciences. Avidin from egg white was purchased from Sigma Aldrich. Avidin beads were purchased from Thermo Fisher Scientific.

Recombinant proteins

cDNA encoding rat syt-I (G374 version) was kindly provided by G. Schiavo (Imperial Cancer Research Fund). The following syt fragments were employed: C2AB (intact cytoplasmic fragment of syt containing tandem C2 domains, residues 96–421), C2A (the first C2 domain of syt, residues 96–265), C2B (the second C2 domain of syt, residues 248–421), C2AA (two identical copies of C2A domains (residues 142–263) connected by the native linker between C2AB (residues 264–272), as described[1]), C2BB (two identical copies of C2B domains (residues 273–421) connected by the native linker between C2A and C2B of syt (residues 264–272), as described[1]). Point mutations were generated using a QuikChange Site-Directed Mutagenesis Kit (Stratagene).

For fluorescence studies, the lone native cysteine (Cys277) in C2AB was substituted with an alanine to generate a cysteine-less template. Then, a single cysteine was introduced at different surfaces of C2B, as indicated in the figures.

All cytoplasmic fragments of syt were subcloned into pGEX-2T or -4T-1 vectors, expressed as glutathione S-transferase (GST) fusion proteins and purified using glutathione-Sepharose beads as described previously[2]. Recombinant syt has been shown to bind tightly to nucleic acid contaminants that affect its properties[3,4]. These contaminants were removed by washing bead-immobilized GST proteins twice with 35 ml of high-salt cleaning buffer as described previously[2]. Soluble syt fragments were generated via thrombin cleavage.

cDNA to generate the C2 domain (residues 17–141) of human $cPLA_2$ was kindly provided by R. Williams (University of Cambridge). Recombinant $cPLA_2$-C2 was expressed as N terminal his_6-tagged fusion protein in *E. coli*. Bacterial pellets were collected, sonicated, and treated with Triton X-100 for 2 h. Insoluble material was removed by centrifugation and the fusion protein was purified from the supernatant using HisTrap HP beads (GE-Amersham). Potential nucleic acid contaminants were removed as described above. The protein was eluted with 500 mM imidazole, and dialyzed overnight at 4 °C against 25 mM HEPES-NaOH, pH 7.4, 100 mM NaCl, 10% (w/v) glycerol.

Plasmids encoding mouse SNAP-25B–rat syntaxin 1A t-SNARE heterodimer and mouse synaptobrevin were kindly provided by J.E. Rothman (Yale University). SNARE proteins were expressed and purified as described previously[5,6]. For individual t-SNARE proteins, cDNA for full-length syntaxin-1A and full-length SNAP-25B were kindly provided by R.H. Scheller (Genentech) and M.C. Wilson (University of New Mexico), respectively. Each t-SNARE cDNA was subcloned into a pTrcHis vector (Invitrogen), resulting in an N-terminal his_6 tag, and proteins were purified as described previously[7].

Liposomes

Protein-free SUVs were prepared by extrusion as described[1]. Briefly, lipids were mixed and dried under nitrogen and lyophilized for 1 h. The dried lipid film was resuspended in HEPES buffer (50 mM HEPES-NaOH, pH 7.4, 100 mM NaCl), and extruded 20 times through 50 nm polycarbonate filters. For all the experiments using protein free SUVs, the lipid composition was 15% PS + 30% PE + 55% PC unless otherwise indicated. For some experiments, fluorescent PE or biotin-PE were also incorporated into vesicles. SNARE-

bearing SUVs were prepared as described previously[8] using 15% PS + 30% PE + 55% PC for t-SNARE vesicles and 15% PS + 27% PE + 55% PC + 1.5% NBD-PE + 1.5% rhodamine-PE for v-SNARE vesicles.

Fluorescence measurements

Membrane penetration assays and FRET experiments were performed at room temperature using a PTI QM-1 fluorometer (South Brunswick, NJ) and FELIX software. NBD-labeled protein was mixed with SUVs (113 μM of total lipid) in a total volume of 600 μl, in the presence of either 0.2 mM EGTA or 1 mM Ca^{2+}. NBD was excited at 470 nm, and the emission spectra were collected from 490 to 630 nm (4-nm slits), and were corrected for blank, dilution, and instrument response. $[Ca^{2+}]_{free}$ was calculated using WEBMAXC STANDARD software (C. Patton, Stanford University). The spectra shown in Figs. 4, 5 and Supplementary Figs. 2–8 were representative from at least two independent experiments.

Liposome aggregation assays

Liposomes were mixed with the indicated concentrations of proteins in a total volume of 1 ml, in the presence of either 0.2 mM EGTA or 1 mM Ca^{2+}. Aggregation was monitored by following the absorbance of liposome suspensions at 400 nm[9] in a BioSpec-1601 UV-visible spectrophotometer (Shimadzu) at room temperature. In order to obtain the pure aggregation signal triggered by Ca^{2+}, the turbidity (Abs_{400nm}) of the vesicle suspension in the presence of EGTA was subtracted from signals obtained in the presence of Ca^{2+}.

Cosedimentation assays

Wild-type or mutant C2AB (2 μM) was mixed with liposomes (1 mM total phospholipids) in the presence of 1 mM Ca^{2+} or 2 mM EGTA, and then centrifuged at 150,000 × *g* at 4°C for 40 min in a Beckman Optima MAX-E (Beckman Coulter) table top ultracentrifuge. The supernatant from each sample was collected and subjected to SDS-PAGE; proteins were visualized by staining with Coomassie blue.

Fusion assays

Fusion between v-SNARE vesicles (Vr) and t-SNARE heterodimer vesicles (Tr) or syntaxin vesicles (SYXr) were carried out as previously described[7] but using 10% the concentration of both vesicles (i.e. 0.5 μl of Vr, 4.5 μl of Tr or SYXr), plus the indicated concentrations of syt, $cPLA_2$-C2 or avidin in a total volume of 100 μl. The mixtures were incubated at 37 °C for 20 min in the presence of 0.2 mM EGTA, followed by addition of Ca^{2+} (1 mM final concentration). Fusion was monitored, as dequenching of NBD fluorescence, for an additional 1 hour. After each run 0.5% of the detergent β-d-maltoside was added to each reaction to solubilize the vesicles, resulting in `infinite' dilution of the NBD-rhodamine FRET pair to produce the maximum fluorescence signal. In this scaled down version of fusion assay, much less syt is required to stimulate fusion as compared to our earlier studies.

Supplementary Material

Refer to Web version on PubMed Central for supplementary material.

ACKNOWLEDGMENTS

We thank members of the Chapman laboratory for their critical discussions and comments during this study. This work was supported by the Howard Hughes Medical Institute (E.R.C.), the National Institutes of Health (NIH) National Institute of Mental Health grant MH061876 (to E.R.C.), and the NIH National Institutes on Deafness and Other Communication Disorders grant 1K99DC011267-01 to C.P.J.

REFERENCES

1. Koh TW, Bellen HJ. Synaptotagmin I, a Ca2+ sensor for neurotransmitter release. Trends Neurosci. 2003; 26:413–22. [PubMed: 12900172]
2. Tucker WC, Weber T, Chapman ER. Reconstitution of Ca2+-regulated membrane fusion by synaptotagmin and SNAREs. Science. 2004; 304:435–8. [PubMed: 15044754]
3. Chicka MC, Hui E, Liu H, Chapman ER. Synaptotagmin arrests the SNARE complex before triggering fast, efficient membrane fusion in response to Ca2+ Nat Struct Mol Biol. 2008; 15:827–35. [PubMed: 18622390]
4. Popoli M, Mengano A. A hemagglutinin specific for sialic acids in a rat brain synaptic vesicle-enriched fraction. Neurochem Res. 1988; 13:63–7. [PubMed: 3368030]
5. Popoli M, Paterno R, Campanella G. Identification and partial purification of a GM1-binding protein from presynaptic vesicles. Acta Neurol (Napoli). 1991; 13:213–9. [PubMed: 1927629]
6. Damer CK, Creutz CE. Synergistic membrane interactions of the two C2 domains of synaptotagmin. J Biol Chem. 1994; 269:31115–23. [PubMed: 7983052]
7. Damer CK, Creutz CE. Calcium-dependent self-association of synaptotagmin I. J Neurochem. 1996; 67:1661–8. [PubMed: 8858951]
8. Arac D, et al. Close membrane-membrane proximity induced by Ca(2+)-dependent multivalent binding of synaptotagmin-1 to phospholipids. Nat Struct Mol Biol. 2006; 13:209–17. [PubMed: 16491093]
9. Connell E, et al. Cross-linking of phospholipid membranes is a conserved property of calcium-sensitive synaptotagmins. J Mol Biol. 2008; 380:42–50. [PubMed: 18508081]
10. Bhalla A, Chicka MC, Tucker WC, Chapman ER. Ca(2+)-synaptotagmin directly regulates t-SNARE function during reconstituted membrane fusion. Nat Struct Mol Biol. 2006; 13:323–30. [PubMed: 16565726]
11. Gaffaney JD, Dunning FM, Wang Z, Hui E, Chapman ER. Synaptotagmin C2B domain regulates Ca2+-triggered fusion in vitro: critical residues revealed by scanning alanine mutagenesis. J Biol Chem. 2008; 283:31763–75. [PubMed: 18784080]
12. Diao J, Yoon TY, Su Z, Shin YK, Ha T. C2AB: a molecular glue for lipid vesicles with a negatively charged surface. Langmuir. 2009; 25:7177–80. [PubMed: 19563216]
13. Garcia RA, Forde CE, Godwin HA. Calcium triggers an intramolecular association of the C2 domains in synaptotagmin. Proc Natl Acad Sci U S A. 2000; 97:5883–8. [PubMed: 10811903]
14. Ubach J, et al. The C2B domain of synaptotagmin I is a Ca2+-binding module. Biochemistry. 2001; 40:5854–60. [PubMed: 11352720]
15. Wu Y, et al. Visualization of synaptotagmin I oligomers assembled onto lipid monolayers. Proc Natl Acad Sci U S A. 2003; 100:2082–7. [PubMed: 12578982]
16. Chapman ER, Davis AF. Direct interaction of a Ca2+-binding loop of synaptotagmin with lipid bilayers. J Biol Chem. 1998; 273:13995–4001. [PubMed: 9593749]
17. Bai J, Tucker WC, Chapman ER. PIP2 increases the speed of response of synaptotagmin and steers its membrane-penetration activity toward the plasma membrane. Nat Struct Mol Biol. 2004; 11:36–44. [PubMed: 14718921]
18. Bhalla A, Tucker WC, Chapman ER. Synaptotagmin isoforms couple distinct ranges of Ca2+, Ba2+, and Sr2+ concentration to SNARE-mediated membrane fusion. Mol Biol Cell. 2005; 16:4755–64. [PubMed: 16093350]
19. Martens S, Kozlov MM, McMahon HT. How synaptotagmin promotes membrane fusion. Science. 2007; 316:1205–8. [PubMed: 17478680]

20. Hui E, Johnson CP, Yao J, Dunning FM, Chapman ER. Synaptotagmin-mediated bending of the target membrane is a critical step in Ca(2+)-regulated fusion. Cell. 2009; 138:709–21. [PubMed: 19703397]
21. Xue M, Ma C, Craig TK, Rosenmund C, Rizo J. The Janus-faced nature of the C(2)B domain is fundamental for synaptotagmin-1 function. Nat Struct Mol Biol. 2008; 15:1160–8. [PubMed: 18953334]
22. Ohki S, Duzgunes N, Leonards K. Phospholipid vesicle aggregation: effect of monovalent and divalent ions. Biochemistry. 1982; 21:2127–33. [PubMed: 7093233]
23. Green NM. Avidin. 1. the Use of (14-C)Biotin for Kinetic Studies and for Assay. Biochem J. 1963; 89:585–91. [PubMed: 14101979]
24. Rufener E, Frazier AA, Wieser CM, Hinderliter A, Cafiso DS. Membrane-bound orientation and position of the synaptotagmin C2B domain determined by site-directed spin labeling. Biochemistry. 2005; 44:18–28. [PubMed: 15628842]
25. Hui E, Bai J, Chapman ER. Ca2+-triggered simultaneous membrane penetration of the tandem C2-domains of synaptotagmin I. Biophys J. 2006; 91:1767–77. [PubMed: 16782782]
26. Connor J, Schroit AJ. Determination of lipid asymmetry in human red cells by resonance energy transfer. Biochemistry. 1987; 26:5099–105. [PubMed: 3663645]
27. Bai J, Wang P, Chapman ER. C2A activates a cryptic Ca(2+)-triggered membrane penetration activity within the C2B domain of synaptotagmin I. Proc Natl Acad Sci U S A. 2002; 99:1665–70. [PubMed: 11805296]
28. Shahin V, et al. Synaptotagmin perturbs the structure of phospholipid bilayers. Biochemistry. 2008; 47:2143–52. [PubMed: 18205405]
29. Wang P, Wang CT, Bai J, Jackson MB, Chapman ER. Mutations in the effector binding loops in the C2A and C2B domains of synaptotagmin I disrupt exocytosis in a nonadditive manner. J Biol Chem. 2003; 278:47030–7. [PubMed: 12963743]
30. Weber T, et al. SNAREpins: minimal machinery for membrane fusion. Cell. 1998; 92:759–72. [PubMed: 9529252]
31. Leslie CC. Properties and regulation of cytosolic phospholipase A2. J Biol Chem. 1997; 272:16709–12. [PubMed: 9201969]
32. Bai J, Wang CT, Richards DA, Jackson MB, Chapman ER. Fusion pore dynamics are regulated by synaptotagmin*t-SNARE interactions. Neuron. 2004; 41:929–42. [PubMed: 15046725]
33. Lynch KL, et al. Synaptotagmin-1 utilizes membrane bending and SNARE binding to drive fusion pore expansion. Mol Biol Cell. 2008; 19:5093–103. [PubMed: 18799625]
34. Chapman ER. How does synaptotagmin trigger neurotransmitter release? Annu Rev Biochem. 2008; 77:615–41. [PubMed: 18275379]
35. Zhang X, Kim-Miller MJ, Fukuda M, Kowalchyk JA, Martin TF. Ca2+-dependent synaptotagmin binding to SNAP-25 is essential for Ca2+-triggered exocytosis. Neuron. 2002; 34:599–611. [PubMed: 12062043]
36. Stein A, Radhakrishnan A, Riedel D, Fasshauer D, Jahn R. Synaptotagmin activates membrane fusion through a Ca2+-dependent trans interaction with phospholipids. Nat Struct Mol Biol. 2007; 14:904–11. [PubMed: 17891149]
37. Lynch KL, et al. Synaptotagmin C2A loop 2 mediates Ca2+-dependent SNARE interactions essential for Ca2+-triggered vesicle exocytosis. Mol Biol Cell. 2007; 18:4957–68. [PubMed: 17914059]
38. Bennett MK, Calakos N, Scheller RH. Syntaxin: a synaptic protein implicated in docking of synaptic vesicles at presynaptic active zones. Science. 1992; 257:255–9. [PubMed: 1321498]
39. Sollner T, Bennett MK, Whiteheart SW, Scheller RH, Rothman JE. A protein assembly-disassembly pathway in vitro that may correspond to sequential steps of synaptic vesicle docking, activation, and fusion. Cell. 1993; 75:409–18. [PubMed: 8221884]
40. Chapman ER, Hanson PI, An S, Jahn R. Ca2+ regulates the interaction between synaptotagmin and syntaxin 1. J Biol Chem. 1995; 270:23667–71. [PubMed: 7559535]
41. Schiavo G, Stenbeck G, Rothman JE, Sollner TH. Binding of the synaptic vesicle v-SNARE, synaptotagmin, to the plasma membrane t-SNARE, SNAP-25, can explain docked vesicles at neurotoxin-treated synapses. Proc Natl Acad Sci U S A. 1997; 94:997–1001. [PubMed: 9023371]

42. Kaetzel MA, et al. Phosphorylation mutants elucidate the mechanism of annexin IV-mediated membrane aggregation. Biochemistry. 2001; 40:4192–9. [PubMed: 11300800]
43. Fernandez-Alfonso T, Kwan R, Ryan TA. Synaptic vesicles interchange their membrane proteins with a large surface reservoir during recycling. Neuron. 2006; 51:179–86. [PubMed: 16846853]
44. Earles CA, Bai J, Wang P, Chapman ER. The tandem C2 domains of synaptotagmin contain redundant Ca2+ binding sites that cooperate to engage t-SNAREs and trigger exocytosis. J Cell Biol. 2001; 154:1117–23. [PubMed: 11551981]
45. Chen YA, Scales SJ, Patel SM, Doung YC, Scheller RH. SNARE complex formation is triggered by Ca2+ and drives membrane fusion. Cell. 1999; 97:165–74. [PubMed: 10219238]
46. Fernandez I, et al. Three-dimensional structure of the synaptotagmin 1 C2B-domain: synaptotagmin 1 as a phospholipid binding machine. Neuron. 2001; 32:1057–69. [PubMed: 11754837]

REFERENCES FOR METHODS

1. Hui E, Johnson CP, Yao J, Dunning FM, Chapman ER. Synaptotagmin-mediated bending of the target membrane is a critical step in Ca^{2+}-regulated fusion. Cell. 2009; 138:709–21. [PubMed: 19703397]
2. Bai J, Tucker WC, Chapman ER. PIP2 increases the speed of response of synaptotagmin and steers its membrane-penetration activity toward the plasma membrane. Nat Struct Mol Biol. 2004; 11:36–44. [PubMed: 14718921]
3. Ubach J, et al. The C2B domain of synaptotagmin I is a Ca^{2+}-binding module. Biochemistry. 2001; 40:5854–60. [PubMed: 11352720]
4. Wu Y, et al. Visualization of synaptotagmin I oligomers assembled onto lipid monolayers. Proc Natl Acad Sci U S A. 2003; 100:2082–7. [PubMed: 12578982]
5. Weber T, et al. SNAREpins: minimal machinery for membrane fusion. Cell. 1998; 92:759–72. [PubMed: 9529252]
6. Tucker WC, Weber T, Chapman ER. Reconstitution of Ca^{2+}-regulated membrane fusion by synaptotagmin and SNAREs. Science. 2004; 304:435–8. [PubMed: 15044754]
7. Bhalla A, Chicka MC, Tucker WC, Chapman ER. Ca^{2+}-synaptotagmin directly regulates t-SNARE function during reconstituted membrane fusion. Nat Struct Mol Biol. 2006; 13:323–30. [PubMed: 16565726]
8. Gaffaney JD, Dunning FM, Wang Z, Hui E, Chapman ER. Synaptotagmin C2B domain regulates Ca^{2+}-triggered fusion *in vitro*: critical residues revealed by scanning alanine mutagenesis. J Biol Chem. 2008; 283:31763–75. [PubMed: 18784080]
9. Ohki S, Duzgunes N, Leonards K. Phospholipid vesicle aggregation: effect of monovalent and divalent ions. Biochemistry. 1982; 21:2127–33. [PubMed: 7093233]

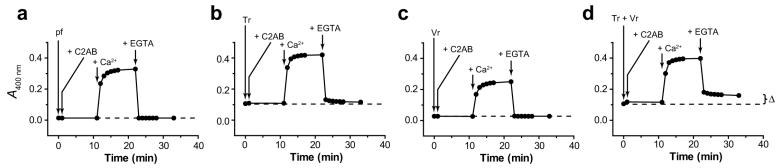

Figure 1.

The cytoplasmic domain of syt aggregates PS-harboring vesicles in a Ca^{2+}-dependent manner. (**a**) Kinetics of turbidity changes (absorbance at 400 nm, A_{400nm}) of the protein-free liposome suspension (designated as "pf") in response to sequential addition of 1 μM C2AB, 1 mM Ca^{2+}, and 2 mM EGTA. C2AB did not cluster vesicles in the absence of Ca^{2+}, but induced rapid and robust liposome aggregation upon the addition of Ca^{2+}; aggregation was rapidly reversed by chelation of Ca^{2+} with EGTA. (**b, c**) The same experiment was performed as shown in (**a**) except using t-SNARE-bearing liposomes (designated as Tr, panel **b**) or v-SNARE-bearing liposomes (designated as Vr, panel **c**). (**d**) Ca^{2+}-dependent, C2AB-mediated aggregation of a mixture of Tr and Vr at a 9:1 molar ratio. In all panels, the total [lipid] was ~113 μM. The Ca^{2+} –C2AB-dependent increases in liposome turbidity were fit with a double exponential function, and the time constant (τ) of the fast component is reported in the text. The "Δ" symbol indicates the irreversible A_{400nm} signal that likely resulted from vesicle fusion. The representative data shown were reproducible in two independent trials.

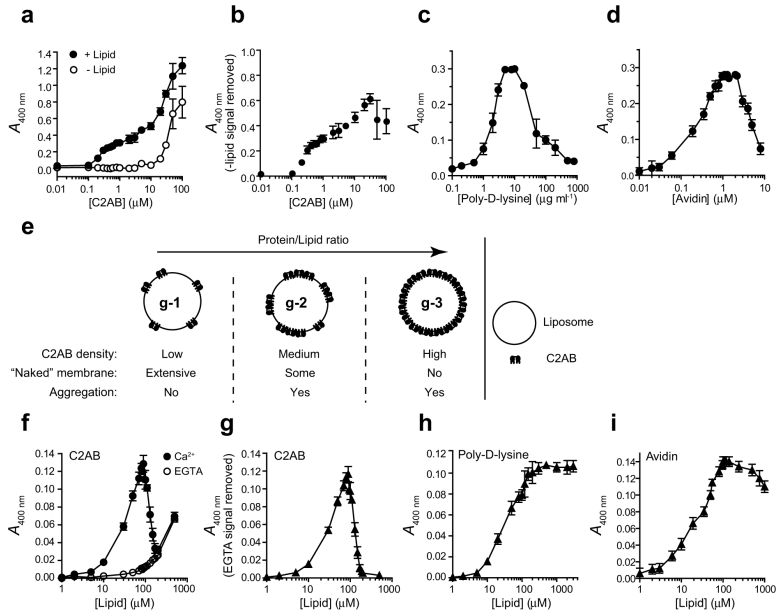

Figure 2.

C2AB aggregates liposomes via a mechanism distinct from avidin-biotin and poly-D-lysine. (**a**) C2AB-mediated liposome aggregation (A_{400nm}) was assayed as a function of [C2AB]. The turbidity was measured 10 min after mixing C2AB and liposomes (113 μM of total lipid), in the presence of 1 mM Ca^{2+} (closed circles). As controls, liposomes were omitted from the mixture and the turbidity measured (open circles). (**b**) The protein-alone aggregation signals were subtracted from the aggregation signals for the protein-lipid mixtures, to obtain corrected signals for C2AB-mediated liposome aggregation. (**c**) Liposome aggregation was assayed as a function of [poly-D-lysine]. (**d**) Avidin-induced aggregation of biotinlylated liposomes (2% biotin-PE) was assayed as function of [avidin]. (**e**) A model summarizing C2AB-mediated liposome aggregation at different protein-to-lipid ratios. The circle indicates a cross-section of a liposome. (**f**) 0.3 μM C2AB was mixed with increasing [lipid], in the presence of either 0.2 mM EGTA or 1 mM Ca^{2+}, and the turbidity was measured 10 min after mixing. Note: at relatively high [lipid], the background turbidity became substantial, leading to an upward deflection in the signal; therefore, all data were corrected. (**g**) Ca^{2+}-C2AB-triggered increases in turbidity were calculated, and plotted against [lipid]. (**h**) 1 μg ml^{-1} poly-D-lysine was mixed with increasing [lipid], and the turbidity of the mixture was measured and plotted as a function of [lipid]. **(i)** 1 μM avidin was mixed with increasing concentrations of biotinylated liposomes, and the turbidity of the mixture was plotted as a function of [lipid]. Data are represented as mean ± s.e.m., n = 3.

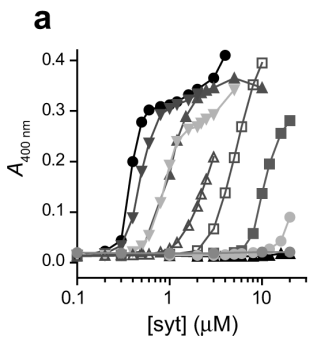

b

Symbol	Protein	Threshold (μM)
●	C2AB	0.2
□	C2AB (D230,232N)	2.0
▽	C2AB (D363,365N)	0.4
●	C2AB (D230,232,363,365N)	> 20.0
●	C2A	12.0
■	C2B	5.0
▲	C2AA	0.5
▼	C2BB	0.3
△	C2AB (R398,399Q)	0.8
▲	C2B (R398,399Q)	> 20.0

Figure 3.

Mutational analysis of syt-mediated membrane aggregation activity. Liposome suspensions containing 113 μM total lipid were mixed with increasing concentrations of protein in the presence of 1 mM Ca^{2+}, samples were incubated for 10 min at room temperature, and the turbidity was measured and plotted as a function of protein concentration for each of the indicated syt mutants. The threshold protein concentration for aggregation was defined as the lowest concentration tested that gave rise to a ≥ 50% increase in turbidity. The representative data shown were reproducible in 2–3 independent trials.

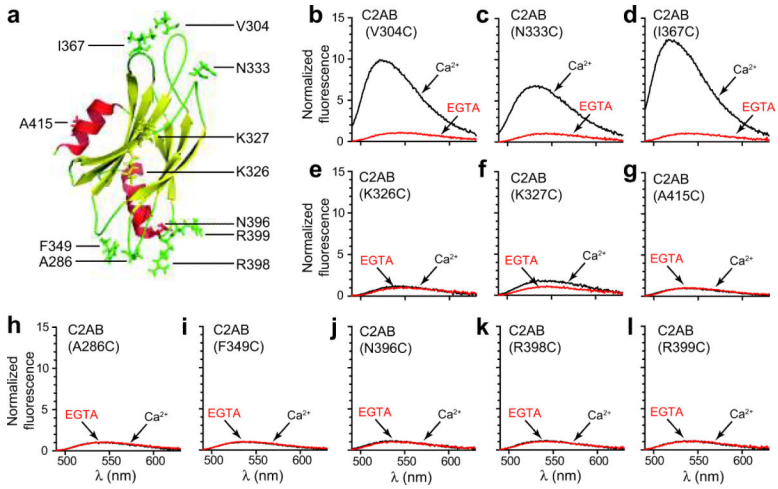

Figure 4.

Mapping the membrane-binding interface of C2B using NBD fluorescence reporters. (**a**) Structural model[46] depicting individual amino acid residues of C2B, in the context of C2AB, that were replaced with cysteines; for simplicity only C2B is shown. The environmentally sensitive fluorophore NBD was used to label each of these sole cysteine residues. (**b–l**) Membrane penetration activity of each residue depicted in **a**. The NBD fluorescence spectrum of each C2AB mutant (0.3 μM) was obtained in the presence of liposomes plus either 0.2 mM EGTA (red) or 1 mM of Ca^{2+} (black). For each mutant, fluorescence was normalized to the peak intensity of the spectrum in EGTA. Ca^{2+} triggered a dramatic fluorescence increase when NBD was placed on the tip of the Ca^{2+}-binding loops, but not when NBD was placed on other surfaces of C2B.

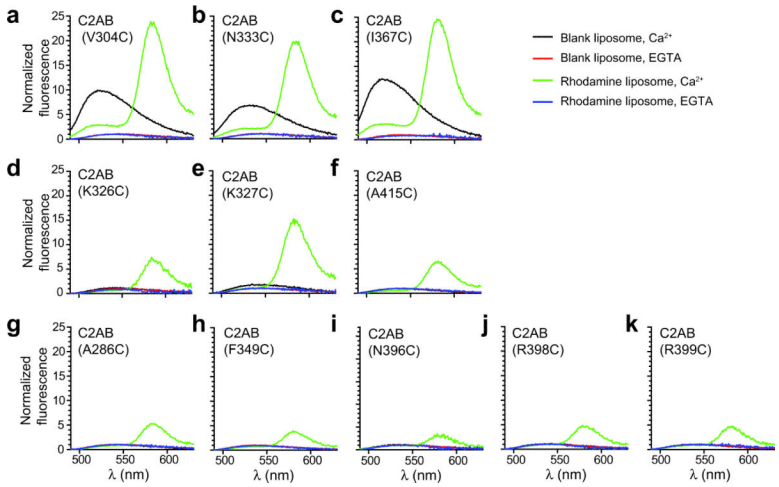

Figure 5.

FRET between NBD-labeled C2AB and rhodamine-labeled liposomes. (**a–k**) Each NBD-labeled cysteine mutant of C2AB (0.3 μM) shown in Fig. 4a was mixed with liposomes that harbored 0.3% rhodamine-PE. Fluorescence spectra were obtained before (blue) and after (green) the addition of 1 mM Ca^{2+}. Mixtures of NBD-labeled C2AB and rhodamine-free liposomes were also tested in parallel as references (EGTA: red; Ca^{2+}: black). For each mutant, all four spectra were normalized to the maximum intensity of samples obtained using rhodamine-free liposomes in EGTA.

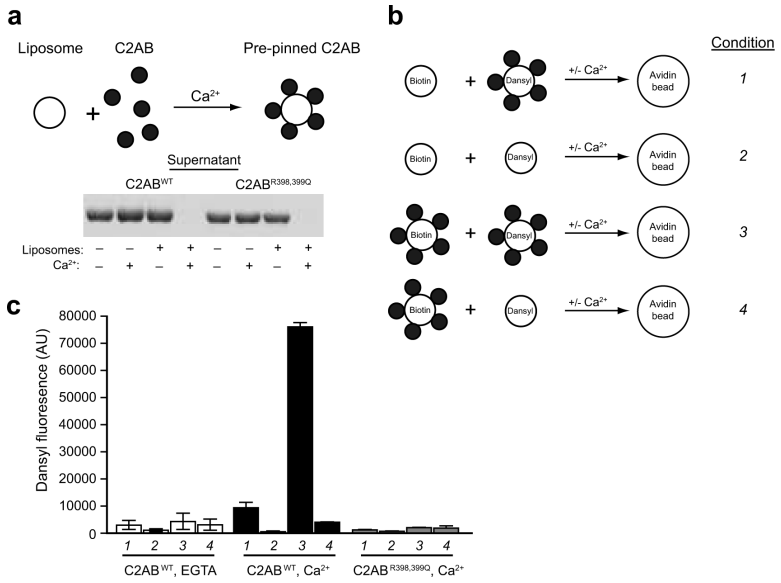

Figure 6.

Syt-mediated vesicle aggregation occurs through *trans* interactions. **(a)** Pre-pinning of C2AB to liposomes. PS-harboring liposomes (1 mM total lipid) were mixed with 2 μM wild-type C2AB or C2AB (R398, 399Q) in the presence of 1 mM Ca^{2+}, and subjected to cosedimentation assays as described in the Methods. Shown is a representative gel demonstrating that both wild-type and mutant C2AB were completely depleted from the supernatant, suggesting complete absorption onto the liposomes. **(b)** Model depicting the experiment. 2 μM C2AB was pre-pinned to liposomes (1 mM total lipid) that harbored 2% of either biotin-PE or dansyl-PE. Immediately after preparation, C2AB-coated liposomes were mixed with either naked liposomes or the other set of C2AB-coated liposomes, in the presence of 1 mM Ca^{2+} or 2 mM EGTA. Avidin beads (30 μl, 50% slurry) were then added to precipitate biotin-PE vesicles - along with any bound dansyl-labeled vesicles - via low speed centrifugation (5000 rpm, 1 min). Beads were washed three times with 500 ml of buffer containing either 1 mM Ca^{2+} or 2 mM EGTA, incubated with 150 μl of n-dodecylmaltoside, and the supernatant was collected and the fluorescence intensity of dansyl determined. **(c)** A bar graph summarizing the dansyl fluorescence of the avidin beads under the conditions indicated. Replacement of wild-type C2AB with C2AB (R398, 399Q) completely abolished the dansyl signal to background levels. Errors bars represent s.e.m., n = 3.

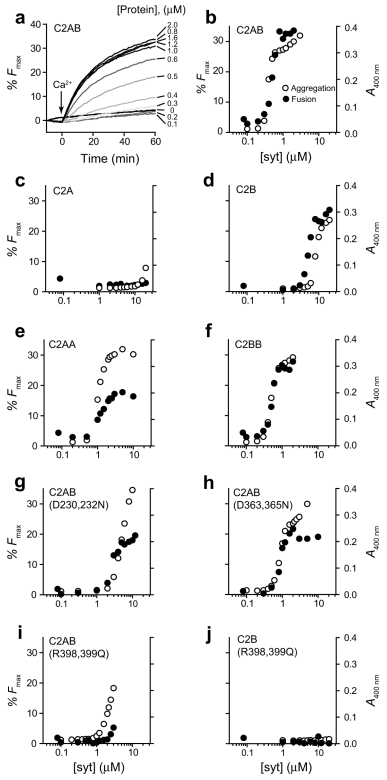

Figure 7.

The ability of syt to aggregate vesicles is correlated with its ability to stimulate fusion of v-SNARE vesicles with t-SNARE heterodimer vesicles. (**a**) Representative NBD de-quenching signals corresponding to fusion between SNARE-bearing vesicles (Tr and Vr) regulated by the indicated concentrations of C2AB. (**b**) The final extent of fusion (closed circles) as shown in **a**, and the degree of aggregation (open circles) as shown in Fig. 3, were plotted against [C2AB] in the same plot. In most cases, vesicle aggregation activity and the fusion-promoting activity of C2AB were closely correlated. (**c–j**) The protein dose-responses for vesicle aggregation and the stimulation of fusion, mediated by each of the indicated syt constructs, were compared. The representative data shown were reproducible in 2–3 independent trials.

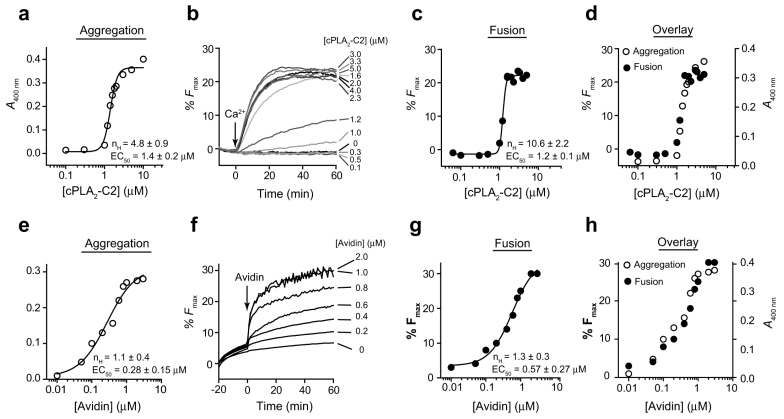

Figure 8.

Stimulation of SNARE-catalyzed fusion by other vesicle aggregating proteins. (**a**) The final extent (at 10 min) of Ca^{2+}-dependent, $cPLA_2$-C2 mediated vesicle aggregation was plotted as a function of [$cPLA_2$-C2]. The turbidity (A_{400nm}) of the vesicle suspension in the presence of EGTA was subtracted from signals obtained in the presence of Ca^{2+}. Data were fit with a sigmoidal dose-response function (variable slope) using Graphpad Prism 5.0 software. (**b**) Representative NBD de-quenching signal corresponding to Ca^{2+}-regulated fusion between SNARE-bearing vesicles (Tr and Vr) in the presence of indicated concentrations of $cPLA_2$-C2. (**c**) The final extent of fusion at 60 min, as shown in **b**, was plotted against [$cPLA_2$-C2]. (**d**) The final extent of aggregation (open circles) and fusion (closed circles) were both plotted against [$cPLA_2$-C2] in the same graph. (**e**) The final extent of avidin-mediated aggregation of biotinylated vesicles was plotted as a function of [avidin]. (**f**) Representative NBD de-quenching signals corresponding to fusion between SNARE-bearing, biotinylated vesicles at increasing [avidin]. (**g**) The extent of fusion at 60 min shown in **g** was plotted against [avidin]. (**h**) The final extent of aggregation (open circles) and fusion (closed circles) were both plotted against [avidin]. Representative data are shown from 2–3 independent trials that yielded similar results.

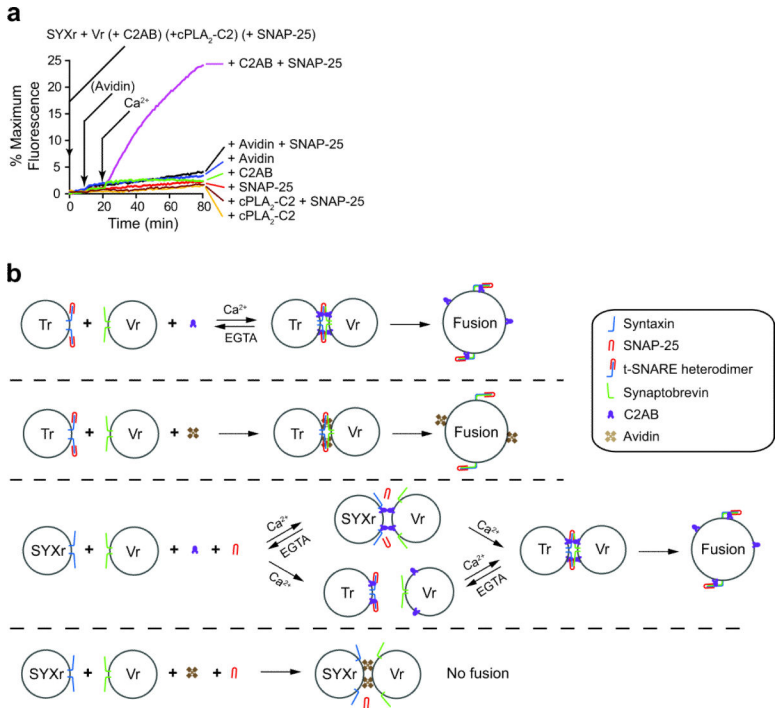

Figure 9.

Ca^{2+}–C2AB, but not other aggregating agents, accelerates fusion between syntaxin bearing vesicles (SYXr) and Vr in the presence of soluble SNAP-25. (**a**) SYXr, Vr and other reactants were added to the reaction at the time points indicated by arrows. In response to Ca^{2+}, C2AB efficiently stimulated fusion of SYXr and Vr in the presence of soluble SNAP-25 (purple trace). Omission of either soluble SNAP-25 or C2AB abrogated the Ca^{2+}-dependent stimulatory effect (green trace and red trace, respectively). Replacing C2AB with avidin or $cPLA_2$-C2 failed to restore regulated fusion. (**b**) Models depicting how Ca^{2+}–syt stimulates fusion of SNARE-bearing SUVs by both aggregating membranes and assembling t-SNARE into fusion competent heterodimers. Shown are representative fusion traces from 3 independent trials.